
STATIC AND DYNAMIC LOAD TESTS ON THE BRIDGE VAHRENDORFER STADTWEG

A PREPRINT

Martin Köhncke 

Chair of Engineering Materials and Building Preservation
School of Mechanical and Civil Engineering
Helmut Schmidt University
Hamburg, Germany
koehnckm@hsu-hh.de

Yogi Jaelani 

Chair of Engineering Materials and Building Preservation
School of Mechanical and Civil Engineering
Helmut Schmidt University
Hamburg, Germany

Alexander Mendler 

Dept. of Materials Engineering
TUM School of Engineering and Design
Technical University of Munich
Munich, Germany

Lizzie Neumann 

Dept. of Mathematics and Statistics
School of Economics and Social Sciences
Helmut Schmidt University
Hamburg, Germany

Philipp Wittenberg 

Dept. of Mathematics and Statistics
School of Economics and Social Sciences
Helmut Schmidt University
Hamburg, Germany

Alina Rode-Klemm 

Chair of Steel Structures
School of Mechanical and Civil Engineering
Helmut Schmidt University
Hamburg, Germany

Sylvia Keßler 

Chair of Engineering Materials and Building Preservation
School of Mechanical and Civil Engineering
Helmut Schmidt University
Hamburg, Germany

ABSTRACT

Load tests are an essential tool to ensure the compliance of bridges with their design specifications. In this paper, a series of static and dynamic load tests on the bridge Vahrendorfer Stadtweg are documented. The bridge is equipped with a long-term Structural Health Monitoring (SHM) system, providing data on an entire seasonal cycle. The objectives of the static and dynamic tests are (i) to capture the bridge's current condition under various loading scenarios while identifying potential structural weaknesses, (ii) to evaluate the system's sensitivity to small mass variations, and (iii) to

generate data for model calibration and validation of anomaly detection algorithms by simulating a design load case. Additionally, the paper conducts plausibility checks on the measurement data and outlines the measurement campaign. In particular, the long-term reference measurements and the time-synchronous additional measurements during the load test have provided an appropriate data set, which can be used in the future to validate finite element models and damage detection algorithms. Follow-up publications will analyze the Structural Health Monitoring (SHM) data in collaboration with multiple research groups. The collected data will also be made available upon request for academic research purposes.

Keywords: Load test, Bridge, Structural Health Monitoring (SHM), Extra mass, Static load test, Dynamic load test.

1 Introduction

Load tests are essential in bridge engineering to ensure the safety and longevity of bridges. Their purpose is to validate design assumptions, calibrate numerical models, assess the vibration intensity, and detect potential issues after the construction or retrofitting. There are two primary types of load tests: Static load tests measure the bridge's response to loads applied gradually or maintained for a period, while dynamic load tests assess the response to loads that rapidly change over time, such as moving trucks. Before tackling the research objectives, a concise literature review on short-term load tests on road bridges is conducted in the following.

Static Load Tests. During static load tests, a stationary load is applied, often in increments, until the structure's static response can be measured (e.g., displacements, inclinations, deflections, strains). The term "static response" means that inertia forces are negligible, that settling effects have subsided, and that low sampling frequencies are sufficient.

The first group of tests are so-called proof load tests, commonly applied to verify design assumptions after the construction. If the test load is smaller than the maximum permissible load, proof load tests are also referred to as target load tests. Here, a newly constructed bridge is loaded to a level that will not be exceeded during normal operations to ensure it can safely carry the expected traffic loads. In Germany, load tests on concrete bridges are often also classified according to the German Committee for Reinforced Concrete guidelines (1). Some countries, such as Italy and Switzerland, require such a test before opening a bridge. Proof load tests may also be effective for bridges that lack structural drawings (2) or to assess the load-bearing capacity of heavily deteriorated bridges (3). The second group of tests is often summarized as diagnostic load tests (4), where known loads are applied for diagnostic purposes and to study the stress-strain relationship. Diagnostic load tests can be applied for various purposes. Firstly, they could be applied to document the structural state of a bridge after construction or rehabilitation for future reference and to assess the effect of time-dependent material degradation by comparing, for example, experimentally determined influence lines to previous states. Secondly, the stiffness or stiffness distribution could be determined for updating analytical bridge models or to estimate distribution factors for load rating (5). Thirdly, diagnostic load tests can be applied to verify serviceability requirements, such as the maximum deflection at midspan (5). Moreover, diagnostic load tests can be applied to quantify load-bearing mechanisms that cannot be accounted for during design, such as arching action (6) or complex shear mechanisms. In bridge design, loads are typically superimposed due to the linearity assumption, and therefore, linearity checks may be performed based on incremental load tests (5). Ultimately, diagnostic load tests are sometimes applied to generate a structural anomaly and validate the effectiveness of structural health monitoring (SHM) systems with permanently installed sensors. Behmanesh and Moaveni (7) applied a 2.29 t concrete weight on the Dowling Hall Footbridge to validate a damage localization and quantification algorithm based on Bayesian model

updating. They are suitable tests to study the performance of uncommon bridge types (e.g., integral bridges) or novel materials, such as carbon-reinforcement concrete, high-performance concrete (8), and lightweight concrete.

Dynamic load tests focus on measuring the bridge's dynamic response (accelerations, velocities, displacements) to loads that change rapidly over time, such as moving trains, trucks, or seismic loads. The system behavior differs significantly from static tests because the sudden load application and resonance phenomena can lead to significantly higher impact loads, and inertia forces have to be considered. Dynamic load tests are suitable for assessing the vibration intensity on bridges (9). For that purpose, the measured accelerations are usually compared to code-based thresholds to guarantee that users do not feel discomfort when passing the bridge on foot or in a truck. Some codes give limiting values of acceleration as a function of the fundamental frequency (10). Another standard problem is the determination of dynamic amplification factors during truck passage (also known as dynamic increment, dynamic load factor, or dynamic coefficient). Burdet and Corthay (10) describe a procedure for estimating the amplification factor in Switzerland based on static and dynamic influence lines, and a more elaborate summary is given by Heywood et al. (3). Furthermore, dynamic load tests are conducted to calibrate bridge weigh-in-motion systems (BWIM). For this purpose, a test truck with known axle geometry and weights is moved across the bridge at different speeds and lanes to verify the experimental influence lines upon which many algorithms are based (11) BWIM systems are most effective for short bridges, and for long-span bridges, the linearity assumption should be verified using static load tests.

Ambiguity in the Nomenclature. Regarding the nomenclature, it is important to distinguish “dynamic load tests” from “dynamic tests” when reviewing the literature on bridge engineering. This is because dynamic testing typically addresses the nature of the system response's nature, not the load. For example, Cunha et al. (12) applied a 60 ton extra mass to the Vasco da Gama cable-stayed bridge. Although the load itself is static, this is considered a dynamic test because the vibrational bridge response is analyzed. Dynamic tests often involve forced vibration tests (based on shakers, hammers, drop-down weights, or snap-back tests) or ambient vibration tests in combination with modal analysis techniques. The resulting natural frequencies, damping ratios, and mode shapes help to assess resonance phenomena and to compare experimentally determined modal parameters to those of a numerical model for dynamic model updating. Another method classified as dynamic testing is the measurement of acoustic emissions. Herein, sound waves are captured during transient fracture processes to detect, localize, and characterize fracture interfaces. In conclusion, one could argue that a characteristic feature of dynamic tests is that inertia and damping forces must be considered and that high sampling frequencies over 100 Hz are required (in case of acoustic emission far beyond 1000 Hz). In contrast, a “dynamic load test” is characterized by dynamic loads, such as those caused by trains, trucks, or wind loads.

Instrumentation. The instrumentation for static load tests consists of strain gauges, displacement transducers, and load cells. Alternatively, contactless measurement systems such as terrestrial laser scanners or other surveying techniques, camera-based systems, and digital image correlation can be used. Accelerometers, seismometers, or contactless systems such as laser Doppler vibrometers are employed for dynamic load tests. The test trucks typically include trucks (loaded with concrete blocks or water tanks), mobile cranes, or military tanks (13), as well as specially designed test trucks with hydraulic jacks, such as the BELFA truck in Germany (14).

This paper applies static and dynamic load tests to the bridge Vahrendorfer Stadtweg, a concrete girder bridge in Hamburg. As part of a greater research initiative, the University of the Federal Armed Forces in Hamburg (HSU) has installed a permanent monitoring system with over one hundred sensors. The objectives of this paper are to (a) document the monitoring system, (b) conduct and document both static and dynamic load tests to capture the current condition state for future reference under various loads, and examine the stress distribution and structural response to

identify potential weaknesses, (c) assess the system's sensitivity to minimal mass variations and (d) generate data for model calibration and validating anomaly detection algorithms by simulating one design load case.

For static testing, Big Bags with sand are placed on the bridge deck, and the load is incrementally increased from 680 kg to 2160 kg in two steps. Moreover, a test truck is parked in various parking positions. The test truck is driven across the bridge at various speeds for dynamic testing. This paper aims to perform plausibility checks on the measurement data and to document the measurement campaign. In follow-up publications, various research groups will analyze the SHM data within and beyond the research cluster.

The remainder of the paper is organized as follows: Section 2, describes the bridge case study, including its monitoring system and numerical model. Section 3 documents the experimental procedure for the static and dynamic load tests, and Section 4 summarizes the preliminary results, followed by the discussion and some conclusions in Section 5.

2 Bridge

2.1 Structure

The bridge Vahrendorfer Stadtweg crosses the A7 German federal highway southwest of Hamburg. The north view of the bridge is shown in Figure 1. It is a prestressed concrete bridge built with an open frame design and a box girder cross-section, constructed in 1972. The bridge has a total length of 50 m and a width of 10 m. It accommodates a single lane for agricultural traffic and a pedestrian walkway. The bridge was initially designed for a traffic load corresponding to Bridge Class 30 as per the German standard DIN 1072 (15), with a permissible axle load of 10 tons. Due to its location and usage, the bridge is expected to experience limited exposure to de-icing salts, which would lead to chloride-induced corrosion and freeze-thaw damage. For this reason, no further investigations or sensors for corrosion measurements were included in the monitoring system. Additionally, carbonation of the concrete may also affect its durability over time.

The longitudinal structure comprises an open frame with cantilever arms on both sides and an arch system. The cross-section features a single-cell box girder with a maximum height of 2.8 m, tapering in an arch-like manner to 1.1 m at midspan. The box girder is accessible via two entry openings. Internal prestressing is installed in both longitudinal and transverse directions and grouted with mortar. Portland cement was predominantly used as a binder for the concrete.

The bridge underwent major refurbishments in 1978 due to construction defects. Additional maintenance measures were carried out in 2010 and 2011, where a surface protection system (OS-C) was applied to the caps. According to inspection reports from 2018 and 2021, the bridge currently exhibits no or only minor defects, such as a 1 cm height offset at the expansion joint and concrete cracks in the caps and frame corners.

2.2 Monitoring system

The SHM system is an important tool in assessing the long-term performance and safety of the bridge structure. The primary purpose of the SHM system is to continuously monitor the structural behavior under various loading conditions, detect early signs of damage or deterioration, and provide close to real-time data that aids in maintenance decision-making and structural reliability assessments.

The monitoring system employs various sensors, including strain sensors, inclinometers, displacement transducers, accelerometers, temperature sensors, and weather stations. Strain sensors are strategically installed to measure the strain on concrete elements in three principal directions (x , y , z), distributed throughout the bridge. Inclinometers



Figure 1: North view of bridge 'Vahrendorfer Stadtweg'.

are positioned at support points to monitor angular changes or tilting, which can indicate alignment shifts or settlement issues. Displacement transducers are installed at expansion joints to capture horizontal displacements, revealing abnormal movements that could compromise the bridge's stability.

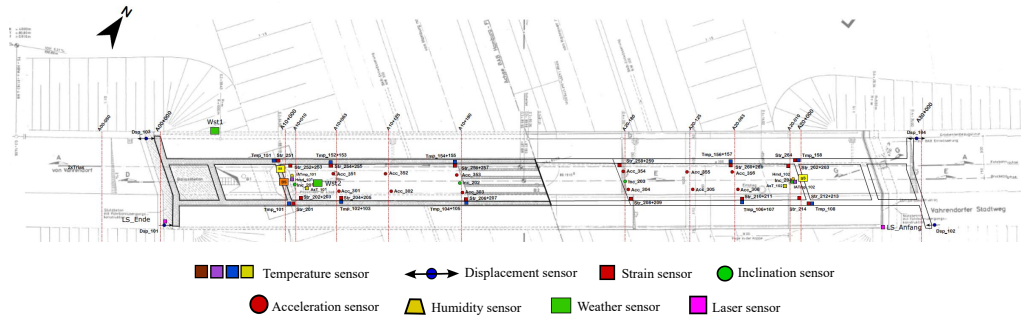
Accelerometers are magnetically mounted on a steel track system, installed beneath the concrete deck, to measure the vibrational response of the structure in three principal directions. The flexibility of the steel track system allows the accelerometers to be repositioned as needed for different research purposes, enabling targeted dynamic assessments. Weather stations are also installed both above and below the bridge to monitor environmental parameters, including air temperature, humidity, wind speed, and direction. Temperature sensors embedded in the concrete elements, the asphalt and in the air of the box girder measure temperature fluctuations, providing insight into how thermal changes may affect the bridge performance, see Table 1 and Figure 2. Thus, the installed monitoring system is well-suited to capturing valuable data during the load tests.

Table 1: Overview of the installed sensors and their sampling rate and mounting.

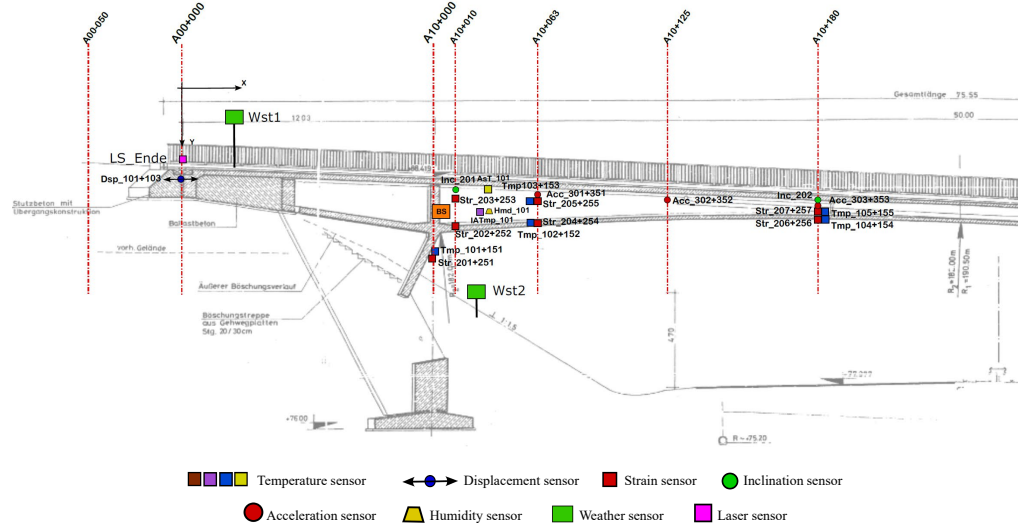
Sensors	Quantity [pcs]	Sampling rate [Hz]	Mounting
Uniaxial accelerometer (Acc_)	36	200	Magnetic
Inclinometer Sensors (Inc_)	8	100	Screw clamp fastening
Strain sensors (Str_)	56	200	Screw clamp fastening
Displacement transducers (Dsp_)	4	100	Screw clamp fastening
Weather stations (Wst_)*	2	10	Externally mounted
Embedded temperature sensors (Tmp_)	18	10	Glued into the structure

*(Wind angle and speed, air temperature, relative humidity, solar radiation)

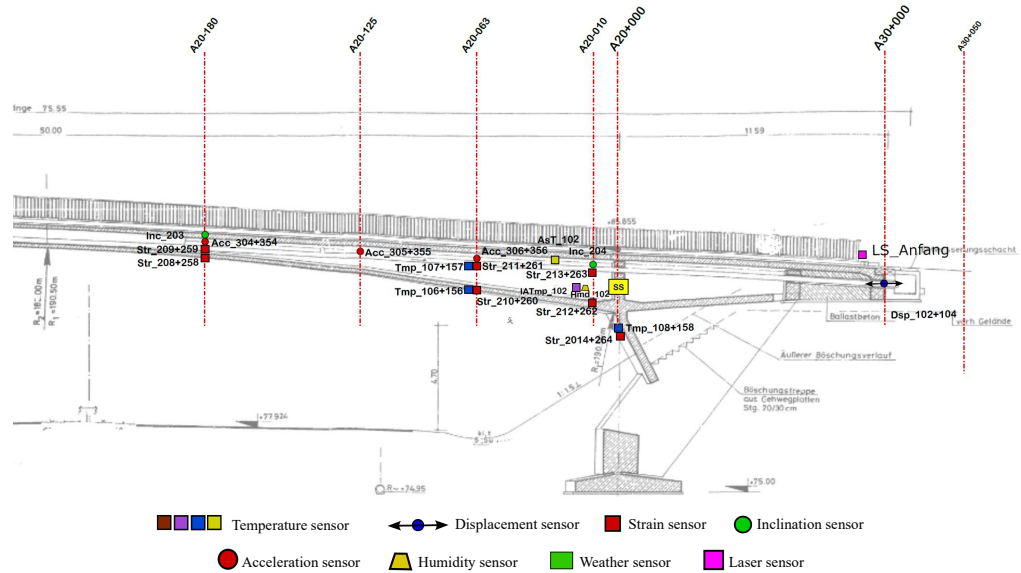
Static and Dynamic Load Tests on the Bridge Vahrendorfer Stadtweg



(a) Top view.



(b) Side view: West side.



(c) Side view: east side.

Figure 2: Instrumentation plan with view from the top (a) and from the side west (b) and east (c).

Three additional laser sensors were temporarily installed for the duration of the load test. One sensor was positioned on the west end to measure in the longitudinal direction of the bridge and monitor the truck’s position during testing. The other two sensors acted as light barriers to calculate the truck’s velocity and accurately record the start and end times of the dynamic load tests. All laser sensors were attached to the railing.

The sensors are named based on their measurement directions relative to the chosen global coordinate system: the X-axis runs longitudinally along the bridge, the Y-axis transversely, and the Z-axis vertically upward. The coordinate origin is located on the western side, centered at the bridge’s roadway crossing.

2.3 Environmental conditions

Environmental conditions are measured above (WST 1) and beneath (WST 2) the bridge. The data collected included global radiation, relative humidity (inside and outside of the bridge), air pressure, precipitation, and temperature (at bridge level, asphalt, and within the structure), cf. Figure 2. Figure 3 shows aggregated hourly measurements and typical seasonal profiles over an entire year, from April 2023 to April 2024, for a selection of sensors. We performed plausibility checks for the ambient temperature data of the weather stations matching with data from the German Weather Service (DWD) at the nearby Rosengarten-Klecken station ID 760 (approx. 9 km away). Wind data was not compared due to its localized nature. Due to the closed hollow box, the relative humidity inside the bridge is relatively stable compared to the reference state measurements. A sharp decrease in the relative humidity of the humidity sensor (inside 1) inside the bridge in June 2023 is caused by the reconfiguration of the monitoring system, including the installation of the second humidity sensor with open access to the hollow box of the bridge.

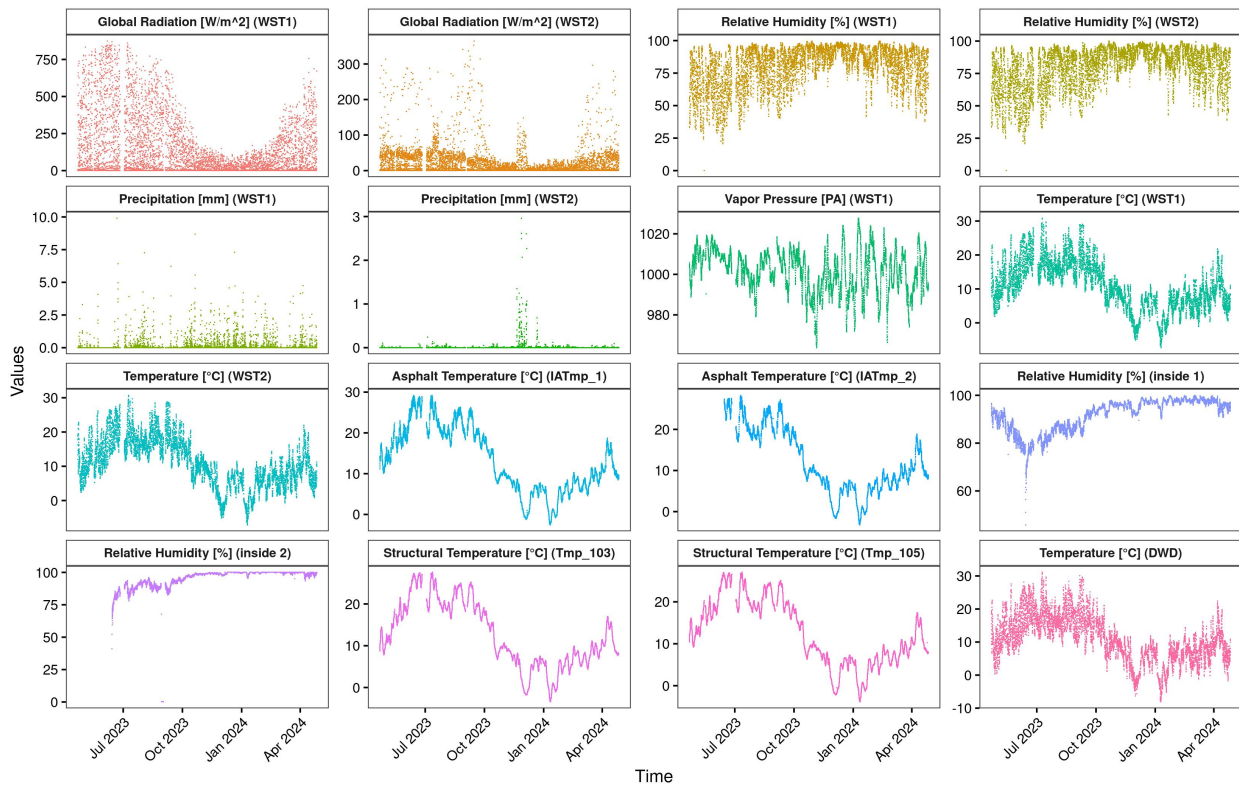


Figure 3: Overview of the bridge’s environmental conditions over a one-year period.

2.4 Numerical system – Digital system

The bridge was modeled using a finite element (FE) approach to predict the performance of the actual structure and simulate various load scenarios. A Building Information Modeling (BIM) system was also developed to centralize and manage information related to the structure and the monitoring system. This BIM model integrates the monitoring data, enabling direct access and visualization of the data through selections within the BIM interface. This setup allows for an intuitive and comprehensive understanding of the structure’s performance, facilitating more effective analysis and decision-making.

3 Experimental procedure for load tests

3.1 Static Load Tests: design and execution

This section outlines the static loading test process’s planning, preparation, and challenges. Two static load tests were conducted:

- Long-Term Static Load Test. Big Bags with sand were placed on the bridge to simulate continuous stress and evaluate performance under prolonged loading.
- Short-Term Static Load Test. A loaded truck was positioned in a stationary parking position on the bridge to simulate continuous stress and evaluate performance under prolonged loading.

The truck, a three-axle truck (A, B, C axles from front to rear, Figure 4), was weighed by the Federal Logistics and Mobility Office in two conditions. When unloaded, it weighed 12.34 t, and when loaded with the trough and Big Bags with sand, the weight increased to 21.25 t. Specific axle loads are shown in Table 2, with all loads within the permissible 10 t per axle, corresponding to the service load level. The short-term static load test was only carried out with the loaded truck. The different short-term static load tests were recorded in separate files to enable load test specific analysis, while the long-term static load test is performed in the standard time step of 5 minute files of the reference state.

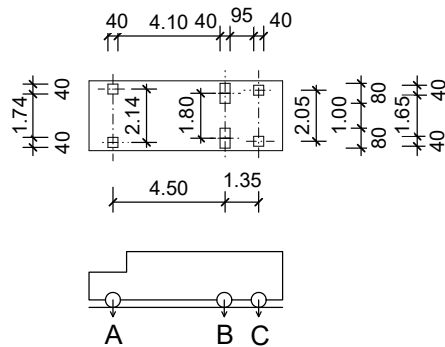


Figure 4: Axle dimensions [m] of used truck.

Axle	Empty weight [t]	Loaded weight [t]
A	6.86	9.34
B	2.82	7.16
C	2.66	4.75
Total weight	12.34	21.25

Table 2: Loads of truck per state.

3.1.1 Long-term static load test: Extra Masses

This test aims to assess the impact of additional masses on monitoring data over time at two bridge positions, accounting for environmental factors and the system’s sensitivity to minimal mass variations. Big Bags with sand (appr.

1600 kg/m^3) were placed initially at the bridge's midpoint on one side of the pedestrian path. The mass was increased in multiple stages: starting with 680 kg (lightweight), then increasing to 1420 kg (mediumweight), and finally to 2160 kg (heavyweight), and each stage was maintained for a ten-day period. The process was then repeated at the bridge's quarter point on the west side, see Figure 5, with specifics in Table 3. The influence of moisture was reduced by enclosing the Big Bags.



Figure 5: The initial additional mass at the quarter point (left) and three additional masses at the center of the bridge (right).

Table 3: Overview of additional masses (in UTC).

Event	Start	End	Added weight [kg]	Position (no.)	Days
light weight	22.02.2024 08:58:00	03.03.2024 06:47:00	680	Middle of the bridge (1)	10
medium weight	03.03.2024 06:47:00	13.03.2024 08:33:00	1420	Middle of the bridge (1)	10
heavy weight	13.03.2024 08:33:00	23.03.2024 08:48:00	2160	Middle of the bridge (1)	10
light weight	23.03.2024 08:57:00	02.04.2024 07:41:00	680	¼ Point of the bridge (2)	10
medium weight	02.04.2024 07:41:00	12.04.2024 07:45:00	1420	¼ point of the bridge (2)	10
heavy weight	11.04.2024 07:45:00	25.04.2024 06:42:00	2160	¼ point of the bridge (2)	14

3.1.2 Short-term static load test: Parking Positions

The truck parking positions were used to simulate the design load case and to calibrate the FE model. The truck was driven to three positions at crawl speed to minimize dynamic effects, as recommended in (16–19). The first parking position was repeated three times for the design load case simulation. At each position in Figure 6 (PP1 in the center, PP2 and PP3 at the western and eastern quarter points, respectively), the truck parked on six steel load distribution plates (400 x 400 mm, 25 mm thick, totaling about 187 kg) for at least ten minutes with the engine turned off. The test truck's driving lane was positioned near the center of the bridge (see Figure 6) to minimize torsional effects. Each test drive was conducted from the east end to the west end of the bridge, with both the starting and ending points located off the bridge. Each position was repeated twice. Parking times are detailed in Table 4 and verified with the data shown in Figure 7. Figure 7 shows the LS_Front laser distance sensor measurement for the first three parking positions. It is easy to see that the distance increases before reaching the parking position, remains constant during this time, and then decreases again after the measurement. The measured times correspond to the data in the overview in Table 4.

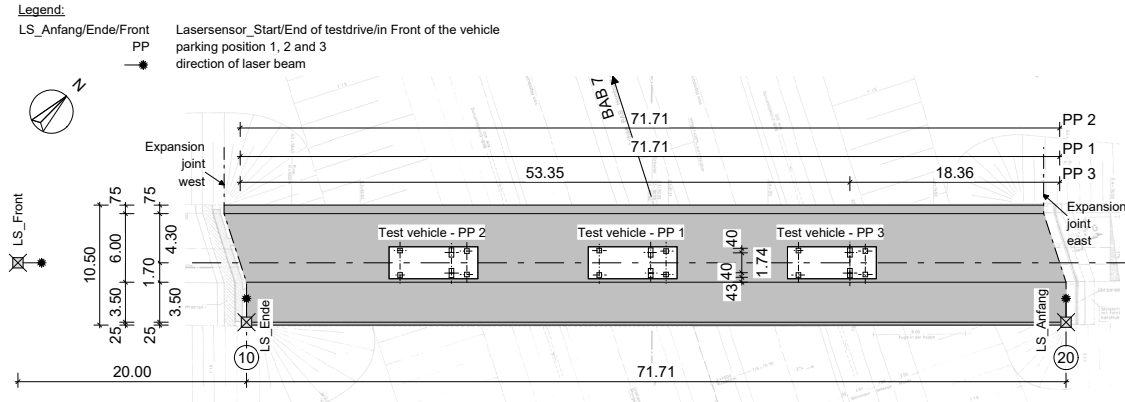


Figure 6: Overview parking positions and laser sensors.

Table 4: Overview of the times of parking positions (in UTC).

Position	Run	Start	End	Details
PP1	1	25.04.2024 12:54.14	25.04.2024 13:04.45	Middle of the bridge
PP1	2	25.04.2024 13:22.12	25.04.2024 13:32.48	Middle of the bridge
PP1	3	25.04.2024 13:43.44	25.04.2024 13:54.20	Middle of the bridge
PP2	1	25.04.2024 14:00.06	25.04.2024 14:10.10	1/4 Point of the bridge (west side)
PP2	2	25.04.2024 14:23.00	25.04.2024 14:33.16	1/4 Point of the bridge (west side)
PP3	1	25.04.2024 14:36.15	25.04.2024 14:47.09	1/4 Point of the bridge (east side)
PP3	2	25.04.2024 14:36.15	25.04.2024 14:47.09	1/4 Point of the bridge (east side)

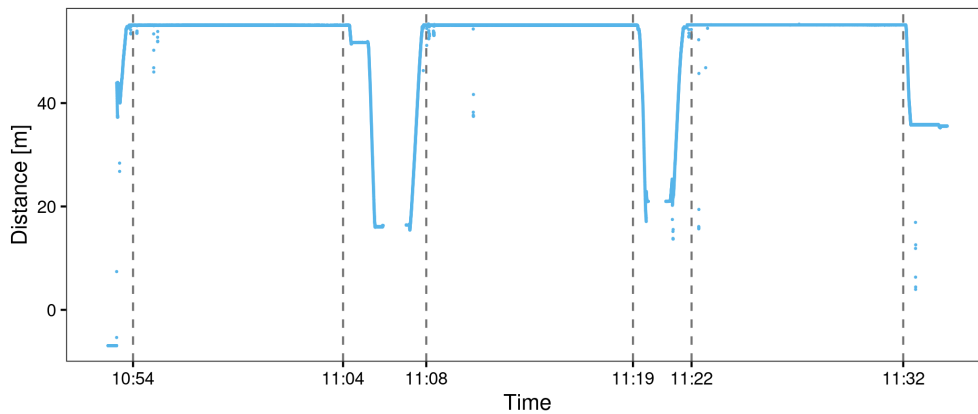


Figure 7: Start and end times of the first three parking positions (each in PP1) for sensor LS_Front.

3.2 Dynamic load test: design and execution

Dynamic load tests assess the bridge’s response to changing conditions, such as vibrations and shifting forces due to moving traffic. The dynamic load test involves driving the loaded and unloaded truck across the bridge at various speeds, maintaining constant velocity to ensure accurate structural response data. Based on experience from tests in the literature (16–19), the following velocities were selected:

- Crawl Speed (5 km/h): Simulates quasi-static conditions, minimizing dynamic effects for baseline data for comparison with higher-speed crossings and the static load test (parking positions).
- 20 km/h: Introduces moderate dynamic effects.
- 40 km/h: Increases dynamic impact further.
- 50 km/h: Tests the maximum speed limit.

Speed levels of 20 km/h and 40 km/h were selected based on references (18, 19) to ensure variability in the dataset with respect to the signal-to-noise ratio and to assess any non-linearity in the response.

Table 5: Dynamic load test speeds and weight combinations.

Truck weight [t]	Speed [km/h]			
	Crawl-Speed	20	40	50
12.34	X	X	-	-
21.25	X	X	X	X

The dynamic load tests are conducted using the truck specified in Table 2 and driving on the same lane as the static load tests (see Figure 6) from east to west. Depending on the speed, deviations in the driving lane in the double-digit centimeter range cannot be ruled out. For the dynamic load test, the combination of the truck’s weight and the corresponding test speeds are summarized in Table 5. The test at Crawl Speed was carried out 10 times in order to minimize the possible uncertainties for comparisons. Each other combination is tested in five separate runs.

4 Preliminary results and plausibility checks

4.1 Static load tests

This section presents the preliminary data analysis results, focusing on plausibility checks across all load test conditions. The evaluation includes strain measurements, inclination data, and horizontal displacements at expansion joints under various scenarios.

4.1.1 Long-term static load test: Extra Masses

For the long-term static load test data involving additional masses, operational modal analysis (OMA) is performed on the 5 minutes interval of vibration data to capture the bridge’s modal parameters in the reference state. Utilizing the Artemis 7.2 software (20), Operational Modal Analysis (OMA) estimates natural frequencies (f), damping ratios (ζ), and mode shapes. Figure 8 depicts the reference state’s global bending and torsional modes from January 8 to January 31, 2024. The results identified the first bending mode at 3.06 Hz and the first torsional mode at 3.95 Hz

Figure 9 illustrates the development of modal parameters, specifically the natural frequency and modal damping ratio, for the first mode during the long-term static load test. This is compared to the bridge’s initial (reference) state without the added mass. Despite adding mass to the bridge, there is only a slight decrease in natural frequency, particularly when the added mass increases to 2160 kg. In contrast to the natural frequency, the damping ratio shows no significant changes, indicating that the added mass did not significantly affect the bridge’s damping characteristic. For this reason, another approach was used to detect the added masses, as described in the following.

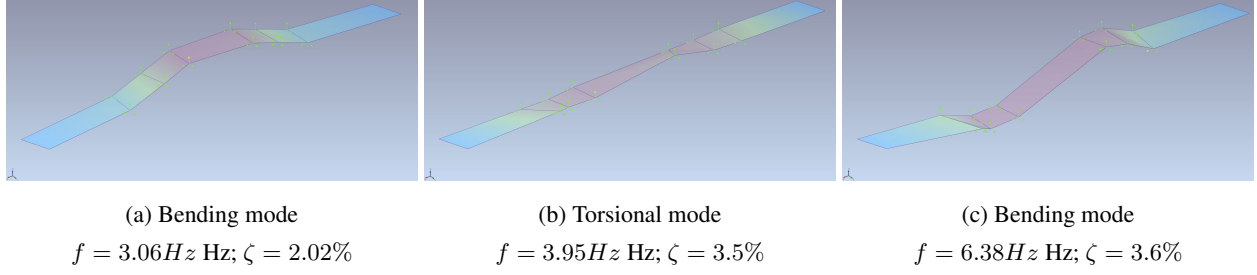


Figure 8: Reference States: a) Global bending, b) torsional, and c) bending modes of vibration.

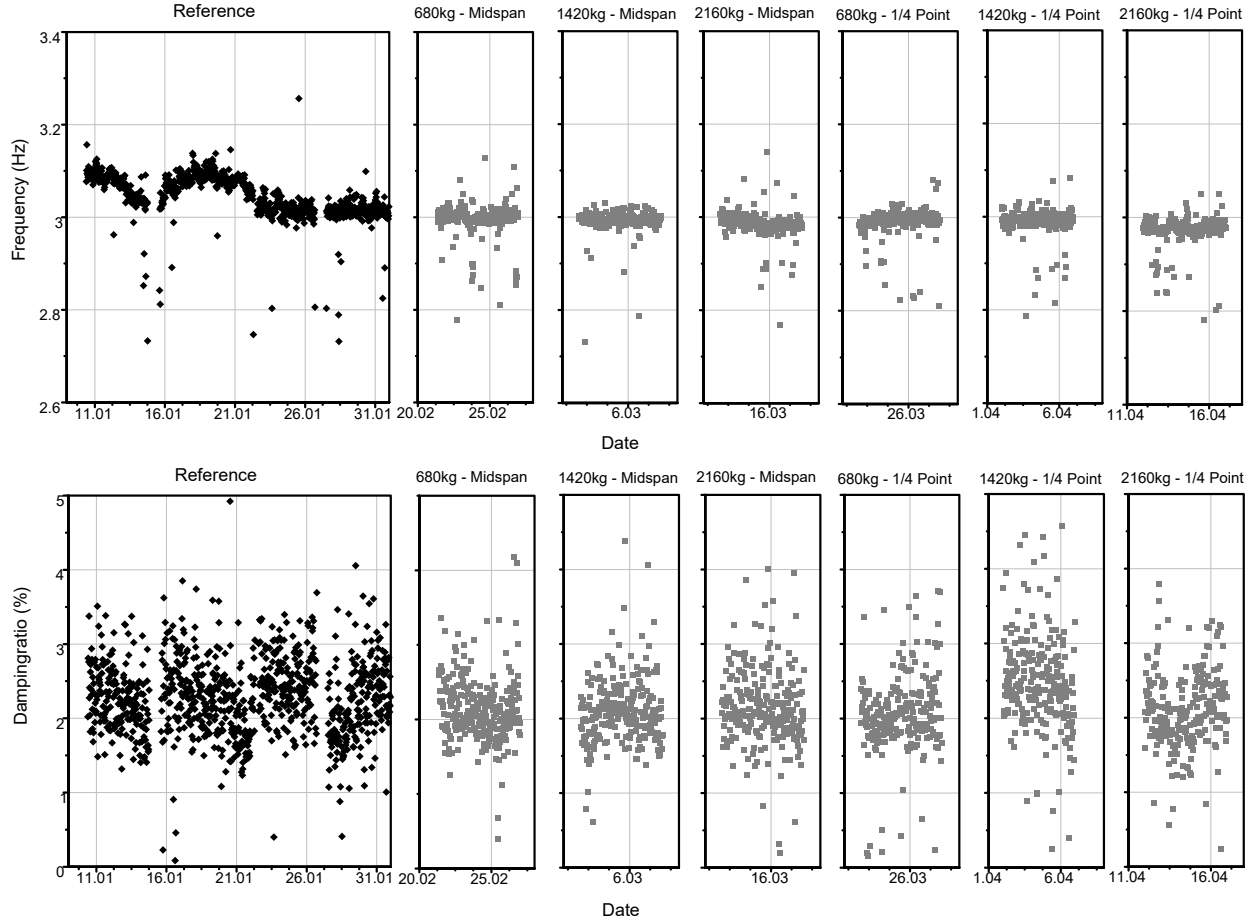


Figure 9: Modal parameters of the first mode in the reference state and during the static load test.

Principal component analysis was chosen to highlight the changes due to extra masses. Six strain sensors were used to estimate the scores and determine if the added masses could be detected. The principal component analysis is shown in Figure 10. The mean, eigenvalues, and eigenvectors were utilized to calculate the scores using the

$$s_i = (\mathbf{x}_i - \boldsymbol{\mu})^\top \mathbf{A} \boldsymbol{\Lambda}^{-1/2},$$

for $i = 1, \dots, n$, where n represents the number of observations, x denotes the measurements, \mathbf{A} is the matrix containing the eigenvectors, and $\boldsymbol{\Lambda}$ is the matrix with the eigenvalues on the diagonal.

The scores are expected to follow a normal distribution. The first column shows the histograms of the first three scores for the reference state without added masses, and the density of the standard normal distribution is added in red color. The second to fourth columns show the histograms of the scores with the added masses at midspan.

In the reference state, the first score exhibits a bimodal distribution due to temperature influences. As discussed in Cross et al. (2012) (21), the first principal component contains the temperature information. However, the second and third scores follow the normal distribution. In contrast, all scores in the “loaded” state deviate from the normal distribution, indicating a mass increase. The procedure can also be applied to other “events” for detection purposes.

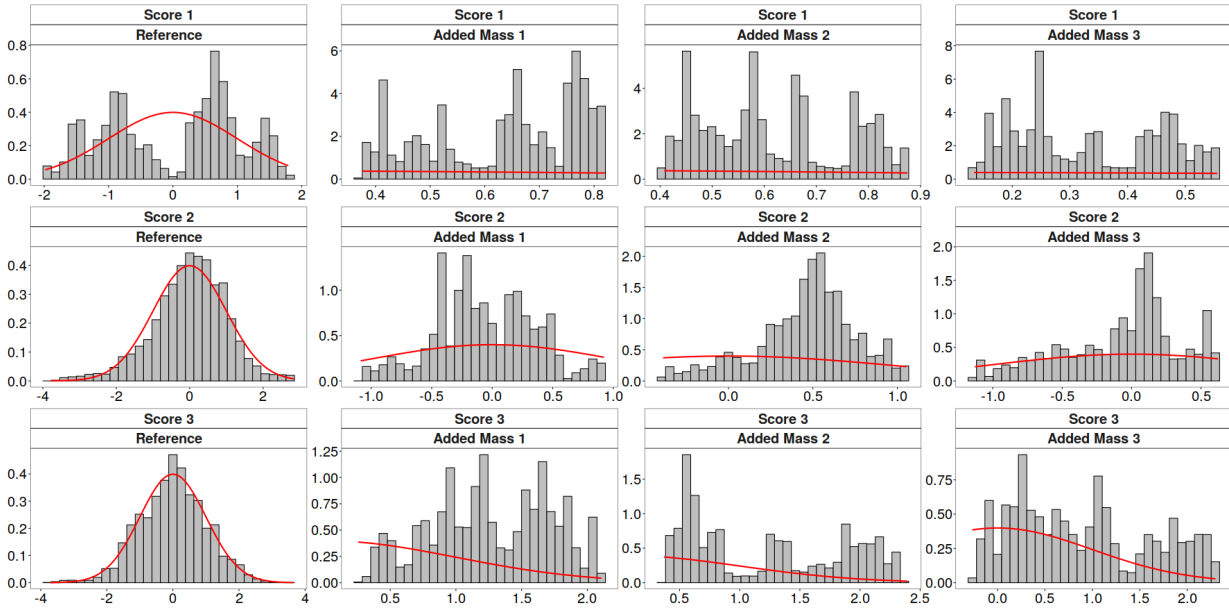


Figure 10: Histogram of Scores (gray) with standard normal density (red).

4.1.2 Short-term static load test: Parking Positions

This section presents the short-term static load test results, focusing on strain, inclination, and displacement at expansion joints to assess the bridge’s response under static loading. The approaches to short-term static load tests from the literature were further developed (18, 19, 22). Especially with regard to the exact positioning of the load for the load tests. The reduction of the measurement uncertainties was implemented by using the mean value of the tests carried out. This was also used when creating the following figures. Signal processing was performed using a Savitzky-Golay filter to reduce noise while preserving essential data integrity for strain, displacement, and inclination. The Savitzky-Golay filter is based on the local least-squares method to smooth short-term fluctuations without disturbing long-term trends (23, 24).

Strain. Since initial strain levels varied across all strain sensors, an offset was applied to standardize comparisons of relative strain changes under different load conditions. Strain data from sensors Str_202Y, Str_203Y, and Str_204Y, located on the web of the concrete box girder near the west abutment, are presented (see Figure 2b). Figure 11 illustrates the strain curve when a 21.25 t truck is parked stationary at midspan. The maximum average strains recorded were $-7 \mu\text{m/m}$ for Str_204Y, $5 \mu\text{m/m}$ for Str_202Y, and $2 \mu\text{m/m}$ for Str_203Y similar to values obtained under crawl-

speed movement, showing consistency between static and dynamic conditions. Additionally, Figure 11 highlights the impact of varying the truck position on the average strain recorded by Str_204Y.

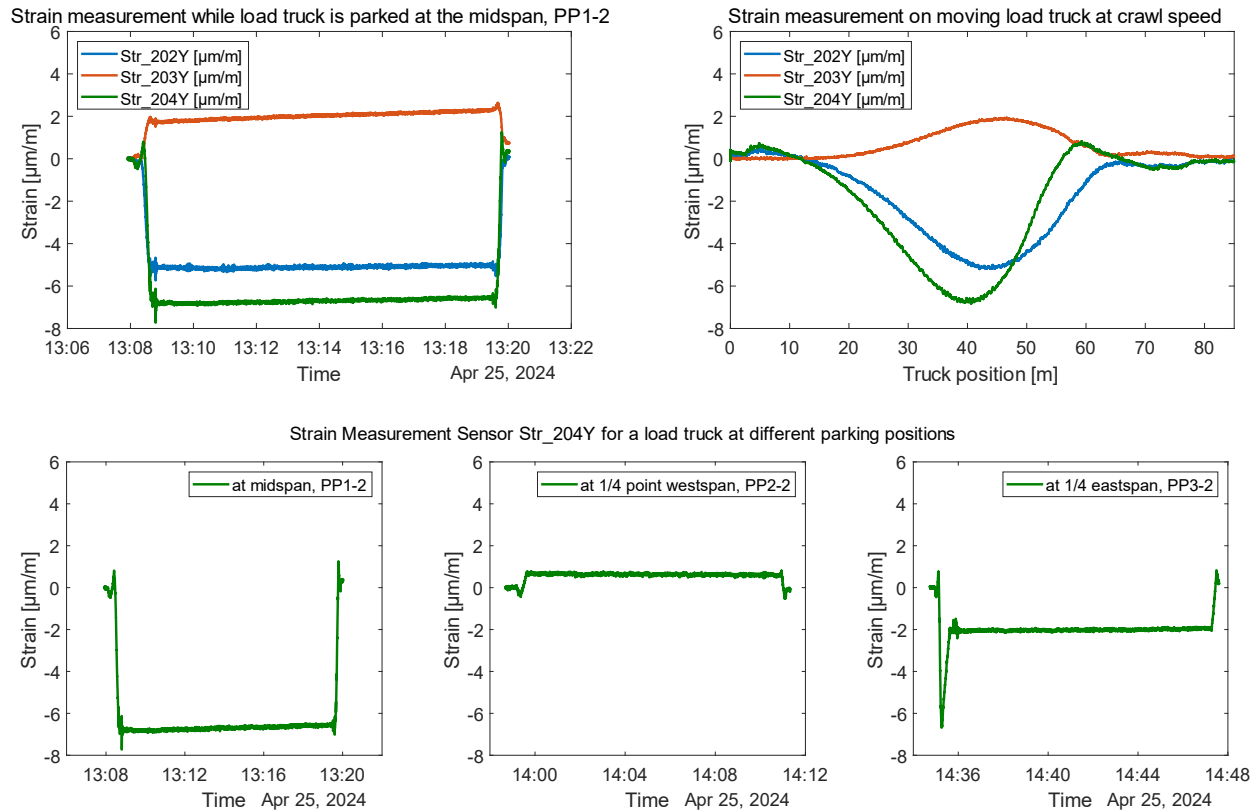


Figure 11: Strain measurement during short-term static load test.

The strain readings' visual plausibility check consistently showed responses confirming the data's reliability and effectiveness.

Displacement. Displacement sensors were grouped by location, with Dsp_101 and Dsp_103 at the western expansion joints and Dsp_102 and Dsp_104 at the eastern expansion joints. Figure 4.2 shows the displacement curve when the 21.25 t truck was stationary at the $\frac{1}{4}$ span on both bridge sections (PP2-2 and PP3-2). The average displacement recorded at the eastern joints was 0.09 mm and 1.10 mm at the western joints, aligning with values observed under the crawl-speed movement of the same truck, indicating consistency between static and dynamic conditions. Horizontal displacement at the joints varied from 0.01 mm to 0.025 mm (up to 25%) during measurements, likely due to temperature fluctuations. The Tmp_103 (west span) and Tmp_107 show only light temperature changes over the measured time. This is why the influence of the temperature change can be considered small.

Inclination. Figure 13 shows the response of inclination sensors 201 and 204 for PP2-2, which are installed near the west and east supports in the X- and Y-directions. The sensors did not exhibit measurable responses, and the inclination sensors detected no significant rotational changes during the short-term static load tests. The signals are indistinguishable from the noise levels. This response is consistent across all loading scenarios.

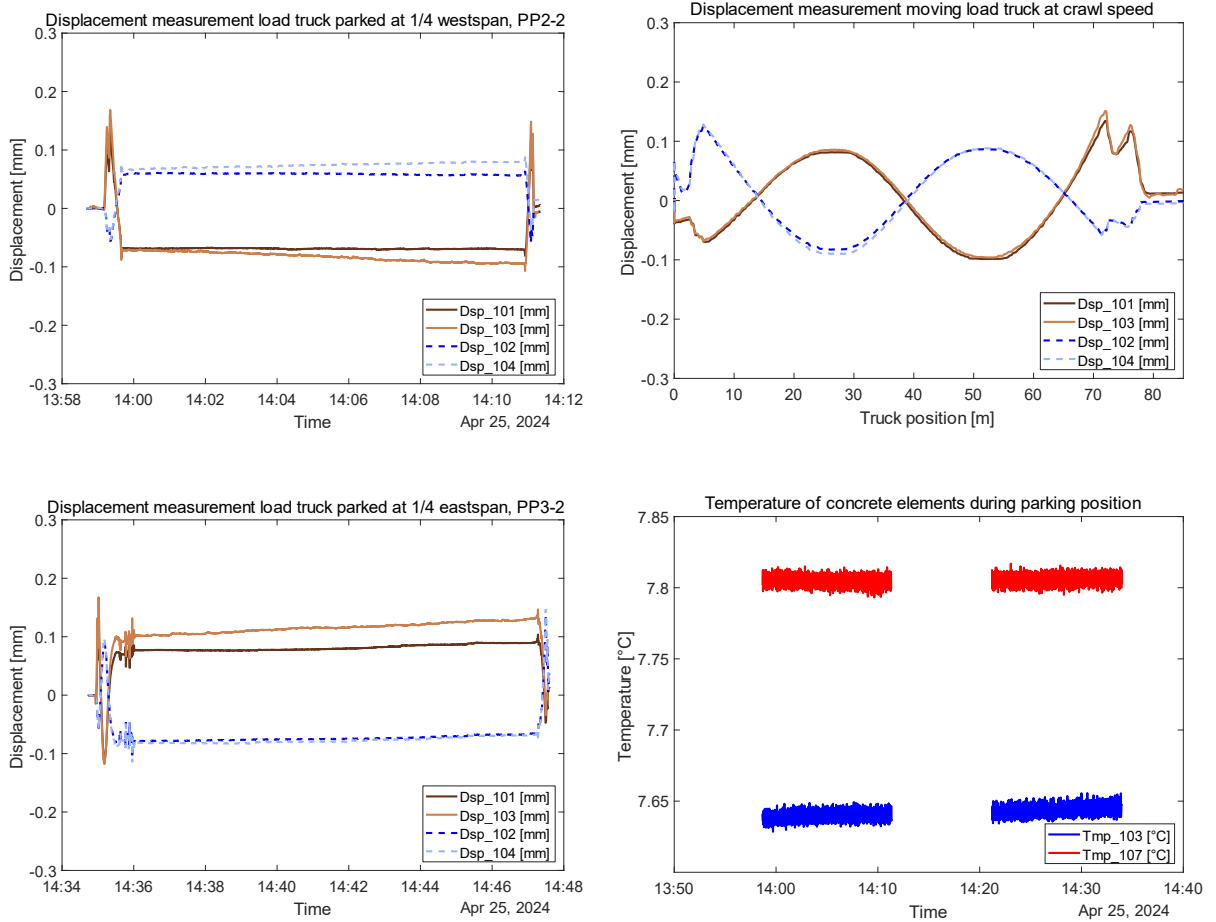


Figure 12: Displacement measurement at expansion joints while a load truck is stationary on the bridge.

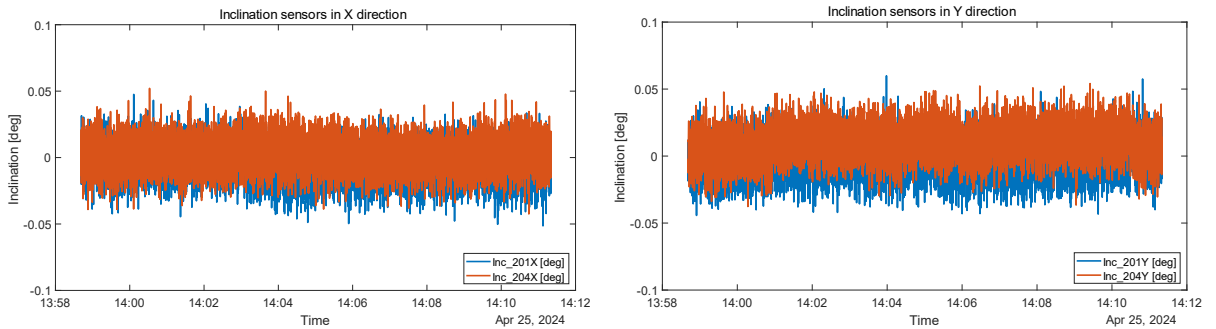


Figure 13: Inclination measurements while the load truck is stationary on the bridge.

4.2 Dynamic Load tests

This section presents preliminary results from the dynamic load test, focusing on strain, inclination, displacement at expansion joints, and acceleration. The analysis assesses the bridge's response to dynamic loading, offering insights into its behavior and performance under varying loads and speeds. The truck crossed the bridge from east to west for

all measurements. During signal preprocessing, a Savitzky-Golay filter is used to reduce noise while preserving data integrity.

Strain. The strain data from selected sensors Str_211Z, Str_205Z, and Str_255Z (which are installed on the web of the concrete box girder, see Figure 2b) are displayed here to compare the strain responses under different speeds and loading conditions. The comparison of the different crossings showed only small deviations between the individual crossings so that only one crossing is shown as an example.

Variation of Speed: Strain comparisons were made between the eastern (Str_211Z) and western (Str_255Z, Str_205Z) sections, as well as between the northern (Str_255Z) and southern (Str_205Z) cross-sections of the structure, see Figure 14. Strain changes from the 21.25 t truck load were consistent across all sensors at different speeds, with no significant dynamic impact observed from higher speeds. Strain levels in the eastern and western sections were similar, around $7 \mu\text{m/m}$. However, a notable difference was found between the northern and southern sections, with the southern strain response being nearly half that of the northern response, likely due to the truck traveling more on the northern side of the bridge than planned.

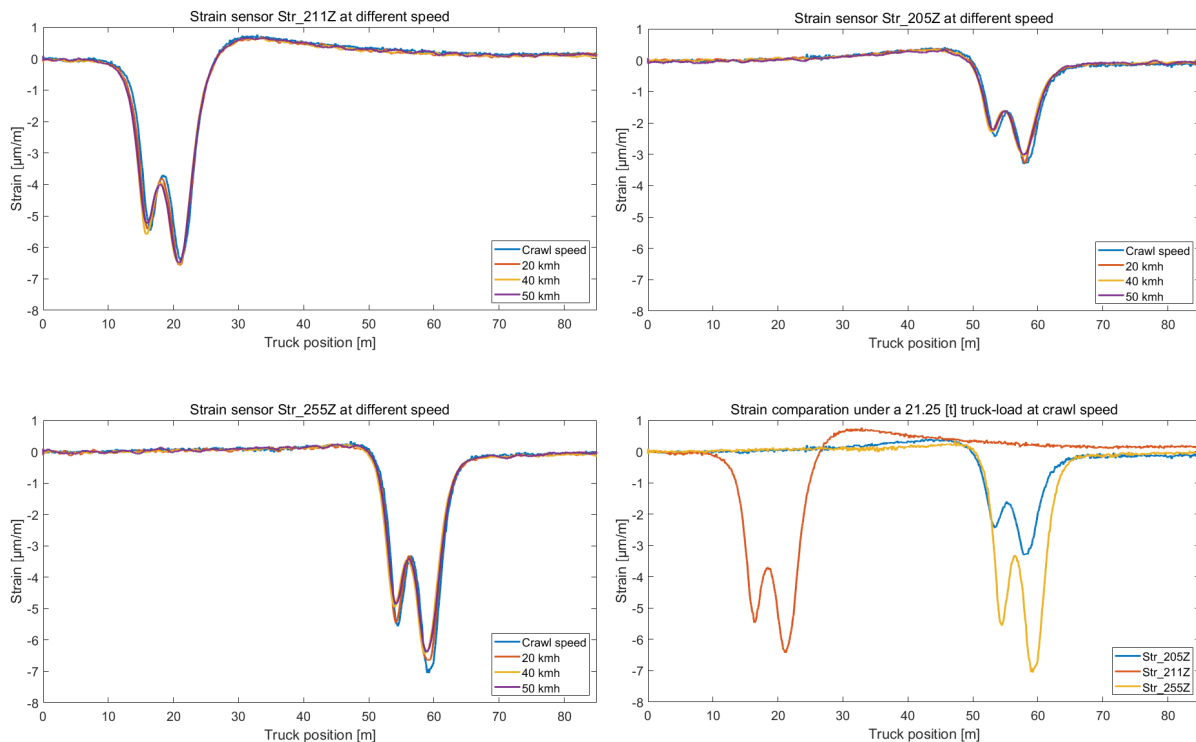


Figure 14: Strain measurements under different speed conditions.

Variation of load at crawl speed: Strain variations are analyzed with different truck weights (12.34 t and 21.25 t) at crawl speeds, see Figure 15. As expected, higher truck loads resulted in higher strain values.

Displacement. The maximum horizontal displacements recorded were 0.15 mm on the west side and 0.13 mm on the east side under a 21.25 t truckload as shown in Figure . Notably, higher speeds did not significantly affect the displacement response, as indicated by constant maximum and minimum amplitudes. At the end of each test, residual displacements were observed: 0.016 mm on the west side and 0.010 mm on the east side. Figure 16 shows displacement variations under different truck weights (12.34 t and 21.25 t) at crawl speeds. Both sensors (Dsp_101

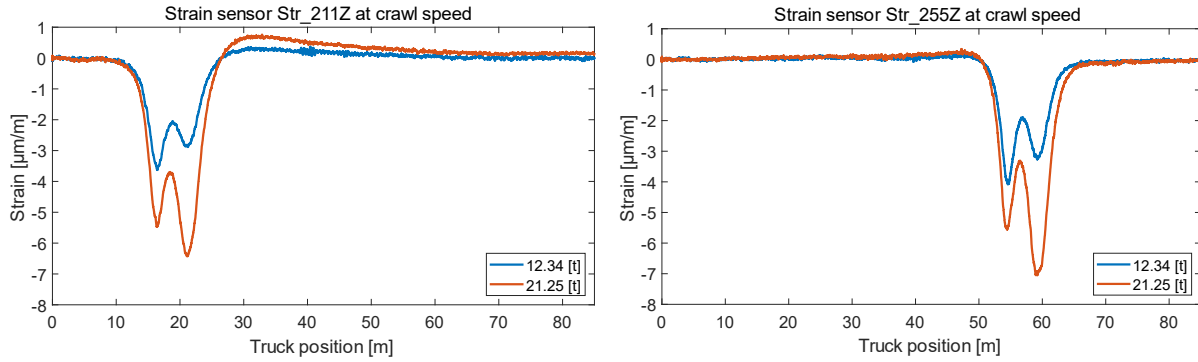


Figure 15: Strain measurement under different truck loads.

and Dsp_102) displayed similar responses to weight variations. As expected, greater truck loads led to increased displacement values.

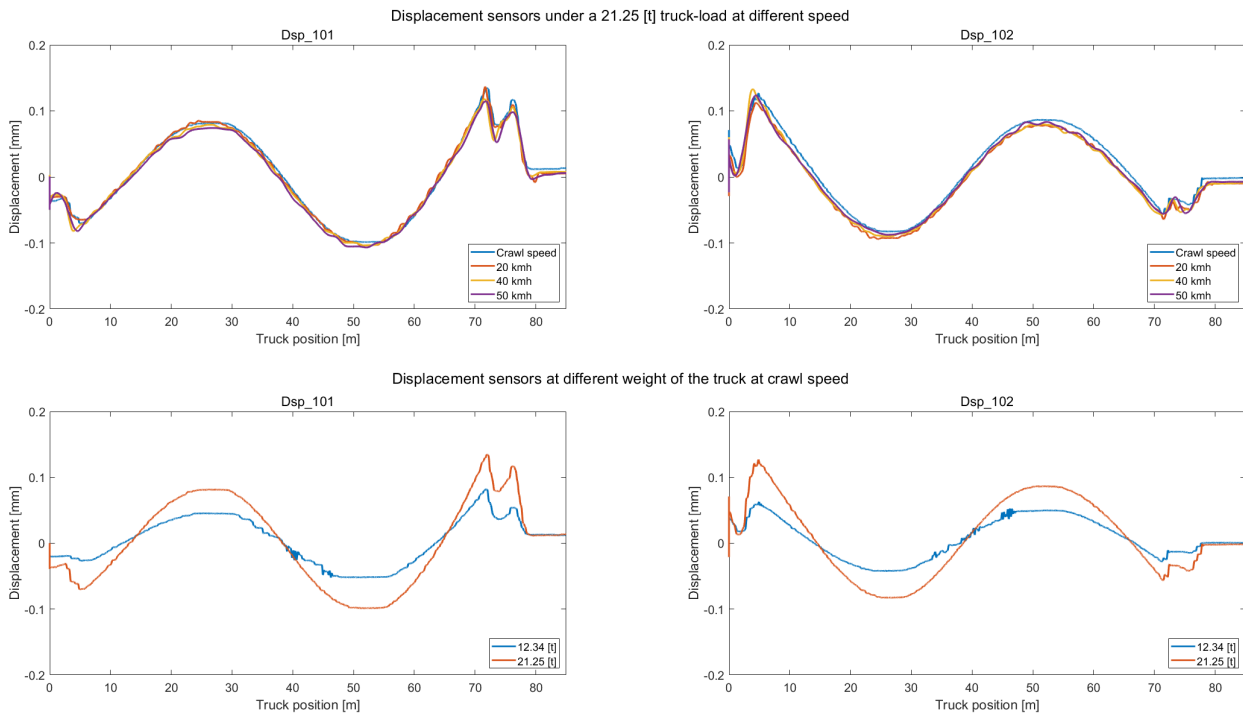


Figure 16: Displacement measurements under different loading scenarios.

Inclination. The inclination sensors did not detect significant changes in bridge rotation during the loading tests, showing no measurable rotational response under various loading conditions. Similar to the static load tests, the signal from the inclination sensors cannot be distinguished from the noise.

Vibration Plausibility checks on vibration data are performed using Fast Fourier Transform (FFT) techniques. The quality of the vibration signals has been ensured by checking for anomalies such as spikes, dropouts, clipping, drifts, and overall signal morphology to meet expected standards. Figure 17 shows a typical vibration signal captured by sensor Acc_353 in the Z-direction at midspan, along with the corresponding frequency spectrum from FFT analysis under different loads and speeds of the truck. This analysis indicates that the dynamic test with the truck successfully

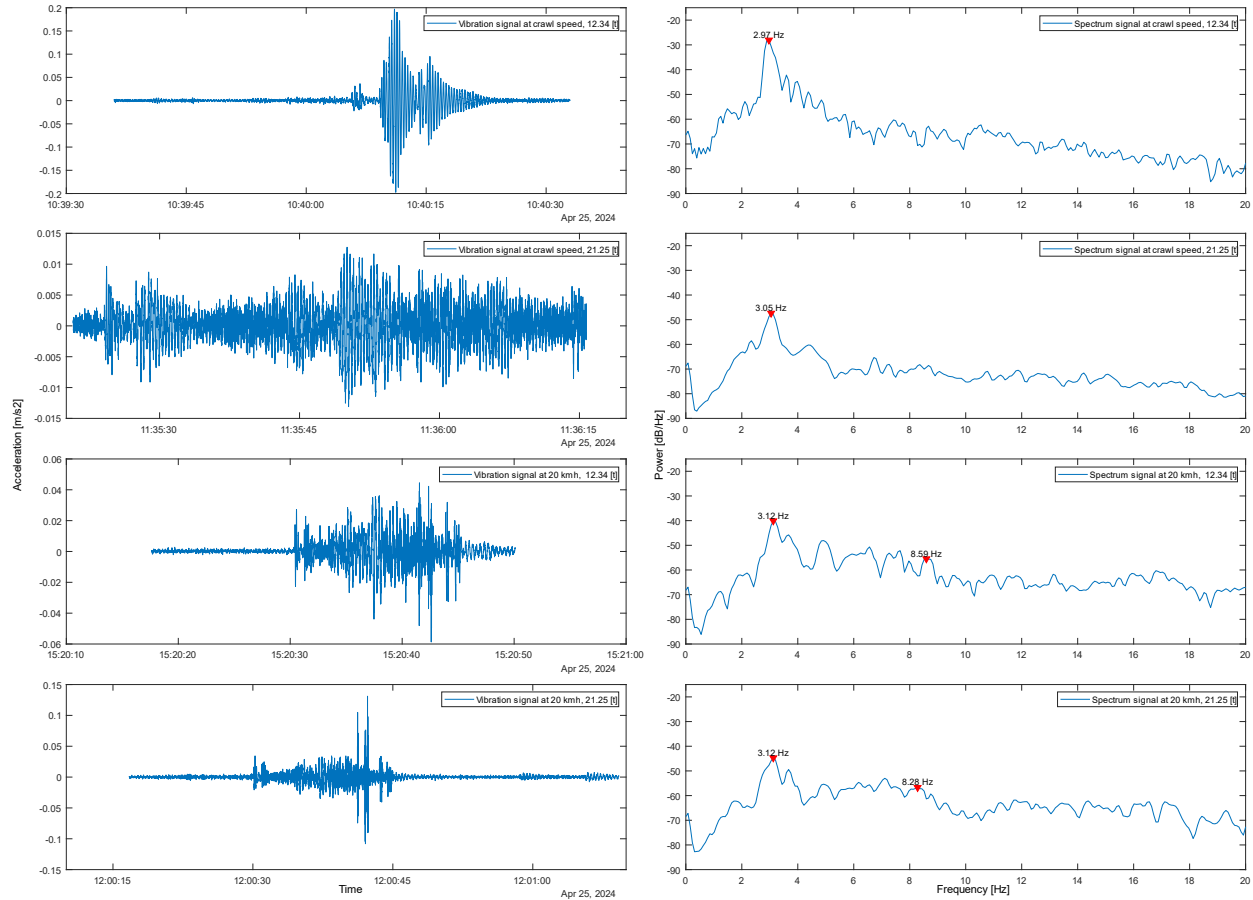


Figure 17: Typical vibration signal sensor Acc_353 in the Z -direction and its corresponding frequency spectrum.

excited at least the first resonance frequency, corresponding to the first natural frequency. This ensures that further dynamic evaluations based on the natural frequencies can be carried out using the generated data.

5 Discussion and conclusions

Following the description of the load test setup and the SHM system, as well as the presentation of data from various load tests, the results are compared with the objectives of the measurement campaign. Examining the static and dynamic load tests captured the current condition for future reference under various loads and analyzed the structural response successfully.

Several key aspects warrant particular emphasis. The truck's movement was captured using laser distance sensors in two ways: first, by recording start and end times with light barriers, and second, by tracking its movement in the direction of travel with an additional laser distance sensor, allowing precise localization of the truck's mass. The redundancy ensures that position detection during measurement is guaranteed even if one sensor fails. The laser distance sensors were temporarily integrated into the monitoring system to synchronize all measurements, facilitating data evaluation. Additionally, the timestamps for each load test are provided to help locate the measurement data within the overall dataset.

The static load tests were conducted over a period of multiple weeks, together with a reference data set of almost one year. By gradually increasing the applied masses, it is possible to assess the minimum detectable mass change, which is particularly useful for damage detection methods that account for temperature variations, such as those described in (25, 26). Score evaluations indicate that even low static loads are sufficient for clear detection, and the high sensitivity of the sensors enables measurements of small loads, around 700 kg.

Dynamic crossings were repeated multiple times, allowing the use of average values for initial assessments. The resulting influence lines confirm that axle loads are readily identifiable, and acceleration values indicate successful excitation of the bridge's first natural frequency. Across different load test scenarios, the inclination sensors showed no measurable response. However, strain values increased approximately linearly with higher truck loads at low speeds, supporting the potential for detailed analysis of structural behavior under varying weights.

These findings suggest that the sensor placement effectively captures loads and natural frequencies. Overall, the results align with the expectations from the load tests and correlate with independently measured environmental parameters. Further analysis will determine the suitability of this data for model calibration and testing additional algorithms for anomaly detection.

Several areas for improvement were identified during implementation. First, increasing the time interval between static and dynamic tests in future load tests would help better differentiate the measurement data and map the starting points more accurately. Additionally, repeating tests at different temperatures would allow for a more direct comparison of temperature effects. Currently, the reference period does not span an entire year, which would be beneficial for thoroughly testing temperature compensation methods.

The analysis of strain sensors revealed that no dynamic amplification could be detected, a finding that requires further investigation as dynamic effects should be measurable according to the literature (10).

In summary, the load tests were successfully conducted and provided a solid foundation for further research. Integrating SHM with load tests offers a valuable approach for validating SHM data and bridge design assumptions. Given the quantity and thorough documentation of the measurements, the data can be used to develop additional algorithms and analyses that correlate various measured parameters. The collected data will also be made available upon request for academic research purposes.

Acknowledgements

This research is funded by dtec.bw – Digitalization and Technology Research Center of the Bundeswehr. dtec.bw is funded by the European Union – NextGenerationEU. We thank all DTEC Project supporters, ATS Alpha Tech Services GmbH, iseatec GmbH, REVOTEC zt GmbH, and the Federal Logistics and Mobility Office (BALM) for providing and weighing the test truck.

Data availability statement

The data that support the findings of this study are available from the corresponding author upon reasonable request.

References

- [1] DAfStb Deutscher Ausschuss für Stahlbeton. *DAfStb-Richtlinie - Belastungsversuche an Betonbauwerken*, 2020.

- [2] Carlos V. Aguilar, David V. Jáuregui, Craig M. Newton, Brad D. Weldon, and Tamara M. Cortez. Load rating a prestressed concrete double t-beam bridge without plans by field testing. *Transportation Research Record*, 2522(1):90–99, 2015. doi:[10.3141/2522-09](https://doi.org/10.3141/2522-09).
- [3] Rob Heywood, Wayne Roberts, and Geoff Bouilly. Dynamic loading of bridges. *Transportation Research Record*, 1770(1):58–66, 2001. doi:[10.3141/1770-09](https://doi.org/10.3141/1770-09).
- [4] Eva O.L. Lantsoght, Cor van der Veen, Ane de Boer, and Dick A. Hordijk. State-of-the-art on load testing of concrete bridges. *Engineering Structures*, 150:231–241, 2017. doi:[10.1016/j.engstruct.2017.07.050](https://doi.org/10.1016/j.engstruct.2017.07.050).
- [5] Chuazhi Dong, Selcuk Bas, Marwan Debees, Ninel Alver, and F. Necati Catbas. Bridge load testing for identifying live load distribution, load rating, serviceability and dynamic response. *Frontiers in Built Environment*, 6, 2020. doi:[10.3389/fbuil.2020.00046](https://doi.org/10.3389/fbuil.2020.00046).
- [6] Susan E. Taylor, Barry Rankin, David J. Cleland, and Jim Kirkpatrick. Serviceability of Bridge Deck Slabs with Arching Action. *ACI Structural Journal*, 104, 2007. doi:[10.14359/18431](https://doi.org/10.14359/18431).
- [7] Iman Behmanesh and Babak Moaveni. Probabilistic identification of simulated damage on the dawning hall footbridge through bayesian finite element model updating. *Structural Control and Health Monitoring*, 22(3):463–483, 2015. doi:[10.1002/stc.1684](https://doi.org/10.1002/stc.1684).
- [8] Yumin Yang and John J. Myers. Live-Load Test Results of Missouri’s First High-Performance Concrete Superstructure Bridge. *Transportation Research Record*, 1845(1):96–103, 2003. doi:[10.3141/1845-11](https://doi.org/10.3141/1845-11).
- [9] Mosbeh R. Kaloop, Mohamed Elsharawy, Basem Abdelwahed, Jong Wan Hu, and Dongwook Kim. Performance assessment of bridges using short-period structural health monitoring system: Sungsu bridge case study. *Smart Structures and Systems*, 26(5):667–680, 2020. doi:[10.12989/sss.2020.26.5.667](https://doi.org/10.12989/sss.2020.26.5.667).
- [10] Olivier Burdet and Stéphane Corthay. Dynamic load testing of swiss bridges. In *IABSE Symposium San Francisco, Extending the lifespan of structures*, pages 1123–1128, 1995.
- [11] Yang Yu, CS Cai, and Lu Deng. State-of-the-art review on bridge weigh-in-motion technology. *Advances in Structural Engineering*, 19(9):1514–1530, 2016. doi:[10.1177/1369433216655922](https://doi.org/10.1177/1369433216655922).
- [12] A. Cunha, E. Caetano, and R. Delgado. Dynamic tests on large cable-stayed bridge. *Journal of Bridge Engineering*, 6(1):54–62, 2001. doi:[10.1061/\(ASCE\)1084-0702\(2001\)6:1\(54\)](https://doi.org/10.1061/(ASCE)1084-0702(2001)6:1(54)).
- [13] Wilmel Varela-Ortiz, Carmen Y. Lugo Cintrón, Gerardo I. Velázquez, and Terry R. Stanton. Load testing and gpr assessment for concrete bridges on military installations. *Construction and Building Materials*, 38:1255–1269, 2013. doi:[10.1016/j.conbuildmat.2010.09.044](https://doi.org/10.1016/j.conbuildmat.2010.09.044).
- [14] Nick Bretschneider, Lutz Fiedler, Gerd Kapphahn, and Volker Slowik. Technische möglichkeiten der probebelastung von massivbrücken. *Bautechnik*, 89(2):102–110, 2012. doi:[10.1002/bate.201100010](https://doi.org/10.1002/bate.201100010).
- [15] DIN e.V. DIN -1072:1967-11, Straßen- und Wegbrücken; Lastannahmen. 1967-11. *Berlin: Beuth-Verlag*, 1967 1967.
- [16] Eva Lantsoght. *Load Testing of Bridges: Current Practice and Diagnostic Load Testing*, volume 12 of *Structures and Infrastructures*. CRC Press, 1st edition, 2019. doi:[10.1201/9780429265426](https://doi.org/10.1201/9780429265426).
- [17] Sreenivas Alampalli, Dan M. Frangopol, Jesse Grimson, Marvin W. Halling, David E. Kosnik, Eva O. L. Lantsoght, David Yang, and Y. Edward Zhou. Bridge load testing: State-of-the-practice. *Journal of Bridge Engineering*, 26(3):03120002, 2021. doi:[10.1061/\(ASCE\)BE.1943-5592.0001678](https://doi.org/10.1061/(ASCE)BE.1943-5592.0001678).

- [18] Maria Schartner, David Sanio, Jan Klinge, Andreas Schmitz, Theres Herzberg, and Manuela Störmer. Monitoring der Theodor-Heuss-Brücke – Teil 2 – Modellbildung und -verbesserung für messwertgestützte Ermüdungsnachweise. *Stahlbau*, 91(4):274–284, 2022. doi:[10.1002/stab.202200005](https://doi.org/10.1002/stab.202200005).
- [19] David Sanio, Jan Klinge, Maria Schartner, Florian Reeh, and Andreas Schmitz. Monitoring der Theodor-Heuss-Brücke – Teil 1 – Veranlassung, Monitoringkonzept und Erkenntnisse zum Tragverhalten. *Stahlbau*, 91(3):172–183, 2022. doi:[10.1002/stab.202100097](https://doi.org/10.1002/stab.202100097).
- [20] *Structural Vibration Solutions A/S. Technical Specifications for ARTeMIS Modal 7.2; 2022 [cited 2024 Nov 11]*. URL https://www.svibs.com/wp-content/uploads/2023/10/ARTeMIS-Modal_tech.-spec._7.2_24.feb_.2022.pdf.
- [21] E. J. Cross, G. Manson, K. Worden, and S. G. Pierce. Features for damage detection with insensitivity to environmental and operational variations. In *Proceedings of the Royal Society A*, volume 486, pages 4098–4122, 2012. doi:[10.1098/rspa.2012.0031](https://doi.org/10.1098/rspa.2012.0031).
- [22] Yogi Jaelani, Alina Klemm, Johannes Wimmer, Fabian Seitz, Martin Köhneke, Francesca Marsili, Alexander Mendler, Max von Danwitz, Sascha Henke, Max Gündel, Thomas Braml, Max Spannaus, Alexander Popp, and Sylvia Keßler. Developing a benchmark study for bridge monitoring. *Steel Construction*, 16(4):215–225, 2023. doi:[10.1002/stco.202200037](https://doi.org/10.1002/stco.202200037).
- [23] Maciej Jan Niedźwiecki, Marcin Ciołek, Artur Gańcza, and Piotr Kaczmarek. Application of regularized savitzky–golay filters to identification of time-varying systems. *Automatica*, 133:109865, 2021. doi:[10.1016/j.automatica.2021.109865](https://doi.org/10.1016/j.automatica.2021.109865).
- [24] Ronald W. Schafer. What is a savitzky-golay filter? [lecture notes]. *IEEE Signal Processing Magazine*, 28(4):111–117, 2011. doi:[10.1109/MSP.2011.941097](https://doi.org/10.1109/MSP.2011.941097).
- [25] Philipp Wittenberg, Lizzie Neumann, Alexander Mendler, and Jan Gertheiss. Covariate-Adjusted Functional Data Analysis for Structural Health Monitoring. 2024. doi:[10.48550/arXiv.2408.02106](https://doi.org/10.48550/arXiv.2408.02106).
- [26] Lizzie Neumann, Philipp Wittenberg, Alexander Mendler, and Jan Gertheiss. Confounder-adjusted covariances of system outputs and applications to structural health monitoring. *Mechanical Systems and Signal Processing*, 224:111983, 2025. doi:[10.1016/j.ymsp.2024.111983](https://doi.org/10.1016/j.ymsp.2024.111983).